



Tan, K.C. and Li, Y. (2001) Performance-based control system design automation via evolutionary computing. *Engineering Applications of Artificial Intelligence* 14(4):pp. 473-486.

<http://eprints.gla.ac.uk/3807/>

Deposited on: 12 November 2007

PERFORMANCE-BASED CONTROL SYSTEM DESIGN AUTOMATION VIA EVOLUTIONARY COMPUTING

K. C. Tan[†] and Y. Li

† Department of Electrical Engineering
National University of Singapore
10 Kent Ridge Crescent, Singapore 119260.
E-mail: eletankc@nus.edu.sg

Centre for Systems and Control, and
Dept. of Electronics & Electrical Engineering
Univ. of Glasgow, Glasgow G12 8LT, UK.
E-mail: y.li@elec.gla.ac.uk

Abstract -- This paper develops a parallel evolutionary algorithm based design unification of linear control systems in both the time and the frequency domains under performance satisfactions. A speedup of near-linear pipelinability is observed for the parallelism implemented on a network of transputers of Parsytec SuperCluster. The approach is capable of tackling practical constraints such as actuator saturation or transportation delays, and can be automated by efficient evolution from plant step response data, bypassing the system identification or linearization stage. Intelligently guided by the evolutionary optimization, control engineers are able to obtain an optimal “off-the-computer” controller by feeding the developed CACSD system with plant I/O data and customer specifications, without the need of formulating a differentiable performance index or linearly parameterization. Validation results against linear and nonlinear physical plants are convincing, with excellent closed-loop responses and good robustness in the presence of practical constraints and perturbations.

I. INTRODUCTION

Over the past few decades there have been great advances in the development of linear control theories and algorithms, ranging from classical proportional plus integral plus derivative (PID), phase lead/lag and pole-placement to more sophisticated optimal, adaptive and modern robust control. Each of these schemes, however, has its own control characteristic or design strategy to tackle a specific class of control problems. For example, a controller designed from the LQR scheme tends to offer a minimized quadratic error with some minimal control effort to overcome actuator saturation, while an H_∞ controller offers robust performance with a minimal mixed sensitivity function to maintain system response and error signals within pre-specified tolerances despite uncertainties. With so many mutually independent schemes available to control engineers, however, an increasing challenge has been imposed to the engineers to select an appropriate control law that best suits the application on hand, and to determine the best controller structure with an optimal parameter set that best meets the performance requirements before any practical implementations are attempted [1-4].

These design deficiencies have prompted the desire of unifying Linear Time-invariant (LTI) control schemes based on performance requirements or customer specifications, eliminating the need of pre-selecting a control law or constrained in a particular design domain [1-4]. With only minor storage and computational overheads, such a performance-prioritised uniform LTI control (ULTIC) can be easily understood and applicable to practical engineers in simplifying their design and implementation tasks. Unlike existing individual LTI control scheme, it is capable of incorporating performance specifications in the time or frequency domains that engineers are familiar with, and takes into account the practical system constraints, such as actuator saturation and time delays.

Developing an ULTIC control system, however, involves simultaneously determining multiple coefficients by optimizing a performance index in a usually noisy and discontinuous multi-modal cost surface. Complexity, nonlinearity and constraints in practical systems, such as voltage/current limits, saturation, noise and disturbance, make the design problem difficult to solve by conventional analytical or numerical means [4-6]. Moreover, the index that reflects practical specifications may not be “well-behaved” and conventional search may only lead to local optimum in the multi-modal multi-dimensional space [5-7]. Although existing modern design succeeds in solving certain class of control problems with derived analytical solutions, these methods only confined to a narrow domain with known limitations such as numerically or physically ill-posed problems, and difficult to take into account the usual hard constraints exist in practical systems [4,8,9]. Such a controller may lead to system degradation or may not realize the full potential of the controller when on-line implementation is performed. Therefore it is difficult to employ conventional methods to achieve a computer-automated design that provides highest possible performance and best meets the customer design specifications automatically.

One possible approach for the design of ULTIC control system is to exhaustively search for all candidate controllers in the solution space. This is, however, practically impossible as an enumerative algorithm requires exponential search time and will thus easily break down due to the high parametric dimensionality of the problems. In contrast, evolutionary algorithm [10,11] that emulating the Darwinian-Wallace principle of “survival-of-the-fittest” in natural selection and genetics, is a polynomial algorithm that improves tractability and robustness in global optimizations by slightly trading off precision in a non-deterministic manner. Such an algorithm can “intelligently” explore, without the need of a differentiable or well-behaved performance index, a noisy and poorly understood space at multiple points by a population of candidate solutions leading to several globally optimized answers. Owing to its good robustness, high efficiency and global capability, the evolutionary

algorithm is naturally suited for ULTIC system design optimization. The EA has been successfully applied to various control applications such as the PID controller design [12,13], pole placement adaptive control [14], linear control [15], optimal control [16,17], nonlinear and sliding mode control [18,19], robust stability [20], fuzzy logic control [21] and neural networks [22,23].

The issues of ULTIC design strategy and its problem formulation in both the frequency and time domain is presented in Section II. Section III illustrates a powerful evolutionary algorithm and its parallelism to achieve design automation of an ULTIC system. Apart from using a model, Section IV shows that the design can equivalently be achieved based on plant input-output (I/O) data directly, bypassing the system identification or linearization stage as required by usual control schemes. In Section V, the applicability of the ULTIC design is demonstrated and implemented on two physical plants, including a multi-input multi-output nonlinear coupled liquid-level system. Finally, conclusions are drawn in Section VI.

II. UNIFICATION OF LTI CONTROL LAWS

Almost all types of LTI controllers are in the form of a transfer function matrix or its bijective state space equation when the design is eventually complete. The order and the coefficients of the transfer function, however, vary with the control law or a single design objective. For example, a μ -controller tends to offer robust performance, while an optimal controller to offer minimum variance of the closed-loop system. Although the obtained coefficients or orders of these two types of controllers may be different, the common purpose of both control laws is to devise an LTI controller that could guarantee a closed-loop performance to meet certain customer specifications in either the time or the frequency domain.

Therefore, a step towards unification of LTI controllers is to coin the design by meeting practical performance requirements, instead of by a specific scheme, or in a particular domain. Thus, a universal LTI controller as shown in Fig. 1 can be described by

$$H(s) = \frac{U(s)}{E(s)} = \frac{a_n s^n + \dots + a_1 s + a_0}{b_n s^n + \dots + b_1 s + b_0} \quad (1)$$

where $a_i, b_i \in \mathfrak{R}^+ \forall i \in \{0, 1, \dots, n\}$ are the coefficients to be determined in the design to satisfy certain specifications; $L^{-1}[E(s)] = e(t)$ is the error input to the controller, the amplitude of which may be restricted by an A/D converter; $L^{-1}[U(s)] = u(t)$ is the controller output voltage with a hard constraint saturation range such as the limited drive voltage or current. In Fig. 1, the plant $G(s)$ to be controlled undergoes a number of perturbations including system time delays, multiplicative perturbations $\Delta_m(s)$ and external disturbance d exist in most practical systems.

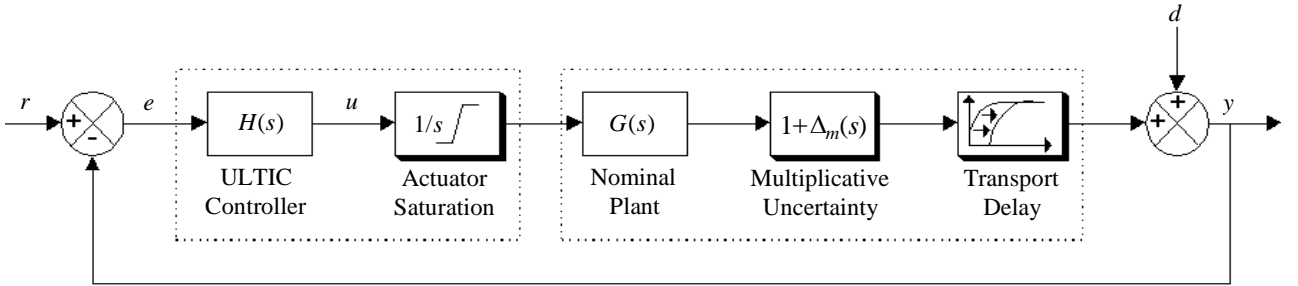


Fig. 1 A practical unity negative feedback control system

The following formalizes the design issue and to develop an evolutionary computation based automated design methodology. The feasibility of unifying classical and modern LTI control strategies in both the time and the frequency domains is reinforced, guided by performance satisfactions. The underlying aim is to let a practicing engineer conveniently to obtain an “off-the-computer” controller directly from customer specifications such as,

Spec. 1: A good relative stability of the closed-loop system (e.g. gain-margin $\in [4 \text{ dB}, 6 \text{ dB}]$, phase-margin $\in [40^\circ, 60^\circ]$ or 3 dB bandwidth $\leq 10 \text{ Hz}$ etc.);

Spec. 2: An excellent steady-state accuracy in terms of small steady-state errors (e.g. s.s.e. $< 3 \%$);

Spec. 3: An excellent transient response in terms of small rise-time, settling-time, overshoots and undershoots (e.g. overshoots < 10 %);

Spec. 4: Robustness in terms of disturbance rejection; and

Spec. 5: Robustness in terms of plant uncertainties.

In order to satisfy various performance requirements, it is necessary to formulate different building blocks in an ULTIC design methodology. Since discontinuous performance index is allowed in evolutionary optimization, other specifications such as noise rejection, economical consideration and etc., may also be added if so desired. These individual building blocks could be added or multiplied to form a composite performance index by either arithmetic or logic operations if specific terms need to be emphasized, which offers an unmatched flexibility over conventional gradient-guided search methods.

A. Basic Performance Index for EA Guidance

In a design exercise, the closed-loop performance can be inverse-indexed conveniently by a basic cost function

$$J_{\min}(H) = N \|e(t)\| \quad (2)$$

or

$$J_{\min}(H) = \|E(j\omega)\| = \|S\| = \frac{1}{1 + H(j\omega)G(j\omega)} \quad (3)$$

Here N is the number of samples used for the simulation and S is known as the sensitivity function. The design task for basic performance is thus to find an optimal coefficient set of $H(s)$ or $\{a_i, b_i\}$ in (1) such that $J_{\min}(H)$ is minimized.

Not that, the design of an LTI controller for an optimal performance can be unified in the time and the frequency domains. It can also be inferred that the design of an ULTIC controller can be carried out in

either the continuous time or the discrete time. The discussions here, however, are restricted in deterministic systems for simplicity, since the ULTIC strategy will be applicable to stochastic systems by involving an expectation operator in the cost function blocks. If the open-loop system is stable, then the Nyquist plot of the denominator of (3) should not encircle its origin in any way. This means that for relatively large stability margins, the denominator plot should be relatively far away from its origin and its magnitude should have a relatively large value. Hence, minimizing the basic index indirectly leads to robust stability and hence largely meets *Spec. 1*.

B. Reconciling Accuracy and Chattering

It is known that smooth control actions often lead to steady-state errors. High control actions usually result in low steady-state errors and high robustness, but also result in chattering and excessive wear of actuators. This may be reconciled by constructing performance index blocks in a similar manner to phase lag-lead compensation or PID control, noting that the chattering is reflected by \dot{e} , i.e., the rate of change of error. Note that index block manipulations can be easily realized in evolutionary guidance, since the EA only requires to compute J_{\min} and not its gradients. To penalize both the error and chattering at the steady-state in the time domain, weighting can be simply realized by multiplying the basic index by simulation time index. Also, weighting this way will not penalize a rapid transient response.

Therefore, the requirements of a high accuracy and low chattering at the steady-state to meet *Spec. 2* and *Spec. 3* can be reconciled in the time domain by adding to the basic index a building block of error derivatives and multiplying them by a building block of time as in

$$J_{\min} = \sum_{t=1}^N [|e_t| + |\dot{e}_t|] t \quad (4)$$

C. Disturbance Rejection

The magnitude of the transfer from the disturbance to the closed-loop output is give by

$$\left\| \frac{Y(j\omega)}{D(j\omega)} \right\| = \left\| \frac{1}{1 + H(j\omega)G(j\omega)} \right\| \quad (5)$$

Therefore, the disturbance rejection is maximized if the basic index or the sensitivity function S is minimized, which largely dealt with *Spec. 4*. In (5), the upper limit of this disturbance rejection is however bounded by the limited control gain due to the actuator saturation. To reflect the level of disturbance attenuation, the following performance weighting function is employed

$$\bar{\sigma}(S(j\omega)) \leq |W_1^{-1}(j\omega)| \quad (6)$$

where $\bar{\sigma}$ defines the largest singular value and $|W_1^{-1}(j\omega)|$ is the desired disturbance attenuation factor.

Allowing $W_1(j\omega)$ to depend on frequency ω enables one to specify a different attenuation factor for each ω in the low frequency.

D. Robustness against Plant Uncertainty

Suppose the nominal plant in Fig. 1 is stable with Δ_M being zero, then according to Small Gain Theorem [24], the size of the smallest stable $\Delta_M(s)$ for which the system becomes unstable is

$$\bar{\sigma}(\Delta_M(j\omega)) = \frac{1}{\bar{\sigma}(T(j\omega))} \quad (7)$$

where $T = GH(1 + GH)^{-1}$ is the complementary sensitivity function used to measure the stability margins of the feedback system in face of multiplicative plant uncertainties. The multiplicative stability margin is, by definition, the “size” of the smallest stable $\Delta_M(s)$ which destabilizes the system shown in Fig. 1. Therefore the smaller $\bar{\sigma}(T(j\omega))$ is, the greater the size of the smallest destabilizing multiplicative perturbation will be and, hence, the greater the stability margins of the system, which largely dealt with *Spec. 5*. The stability margin of the ULTIC system can be specified via the singular value inequalities such as

$$\overline{\sigma}(T(j\omega)) \leq |W_2^{-1}(j\omega)| \quad (8)$$

where $|W_2^{-1}(j\omega)|$ is the respective sizes of the largest anticipated multiplicative plant uncertainties for the high frequency.

III. EVOLUTION ENABLES AUTOMATION

As addressed in the Introduction, evolutionary algorithm is probabilistic in nature and based on *a-posteriori* information obtained by computerized trial-and-error, require no direct guidance and thus no stringent conditions on the cost function. Supported by Schema Theory [25], EA requires an exponentially reduced search time, which could be further speeded up several times if engineers' existing experiences are included in the initial design 'database' for intelligent design-reuse [26]. It is thus particularly useful to provide automated solutions for ULTIC design by incorporating different performance blocks in the optimization as to best meets the need of engineers' design specifications.

Readers may refer to [10,11,25] for detail algorithms of the EA. The multiple search nature of reproduction and evolving population indicates that EAs are a natural parallel paradigm [4,27]. For this, island model parallel EA that has separate and isolated sub-populations that evolve independently and in parallel, with fitter chromosomes occasionally migrate between the sub-populations is studied in this paper. The parallelism is developed under a 64-processor Parsytec transputer system. All simulation tasks in the ULTIC design are equally shared by up to 64 T8 transputers in a 2-D array, which are provided by a Parsytec SuperCluster including the host transputer for communications and supervisory tasks. Parallel C is used under the PARIX (PARAllel unIX) operating system that offers straightforward software-channels for inter-transputer communications.

As illustrated in Fig. 2, conventional “computer-aided control system design” (CACSD) package that provides simulation results is used to evaluate performances of candidate controllers in terms of plant outputs, closed-loop errors and control signal provision. Artificial evolution then enables CACSD to become “computer-automated control system design” [4], where the performances on how well the candidate controllers meet the specification are used “intelligently” to guide the coefficient adjustment. This, however, requires a model of the plant to be controlled in the evaluation process.

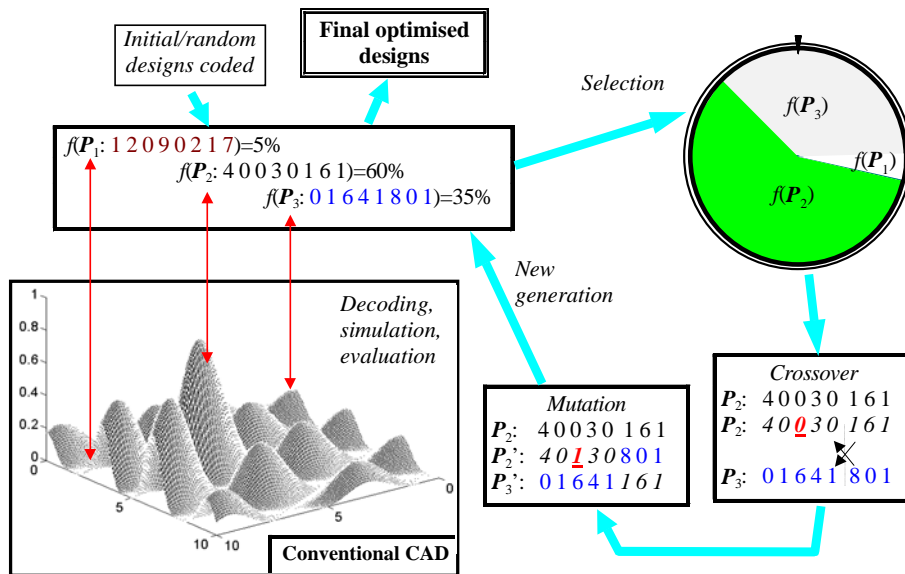


Fig. 2 Evolution automated CACSD by performance evaluations

IV. DIRECT DESIGN FROM PLANT STEP RESPONSE DATA

A. I/O Data Represent a High-Fidelity Model

In many applications, step response data are often obtained when testing or setting the operating point of the system. An LTI model of the plant is then identified or refined from the I/O data before the design of a controller is attempted. An example of plant response data, $y_s(t)$, to a step input of amplitude $A = 3\text{ V}$ are plotted in Fig. 3. A first-order model with transport delay is identified from the data using a curve fitting approach [4,28], as given by

$$G(s) = \frac{K}{1 + s\tau} e^{-Ds} \quad (9)$$

with $K = 0.018$, $D = 1$ s and $\tau = 150$ s.

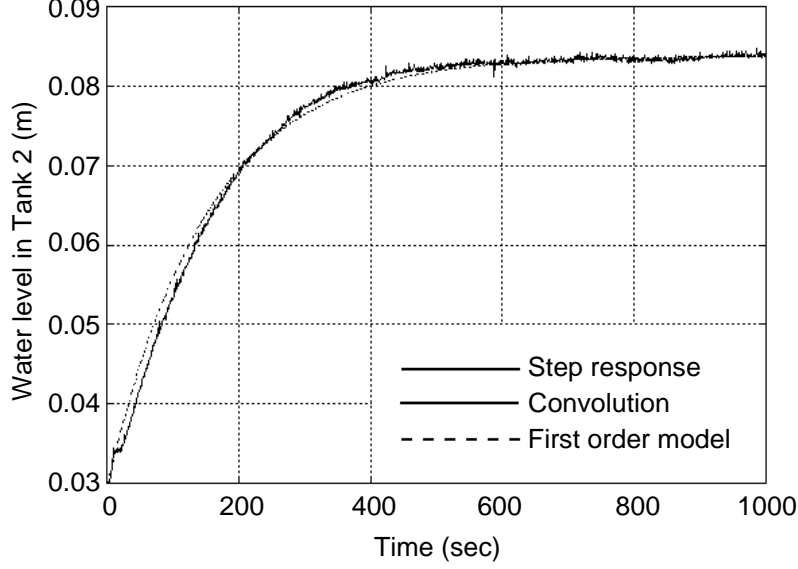


Fig. 3 Plant response data $y_s(t)$ for 3 V input, response of the first-order model and response obtained by convoluting the impulse response

Owing to the simplicity and an acceptable accuracy, in certain control engineering practice, such a linear identification technique is even employed to fit data from a plant that may be internally nonlinear. Partly, this is because many nonlinear plants exhibit the “Type 0” behavior of an equivalent linear system, where all energy storing elements are causal and thus a non-zero control energy is needed to maintain the steady-state operating point as indicated by Fig. 3. It is interesting to note that the step response data were, in fact, obtained from the output $y(t)$ of a nonlinear coupled liquid-level system as shown in Fig. 4. The system simulates the mass-balance dynamics usually found in the chemical and dairy plants with the nonlinear dynamics given by

$$\begin{bmatrix} \dot{h}_1 \\ \dot{h}_2 \end{bmatrix} = \begin{bmatrix} -\operatorname{sgn}(h_1 - h_2) \frac{C_1 a_1}{A} \sqrt{2g|h_1 - h_2|} \\ \operatorname{sgn}(h_1 - h_2) \frac{C_1 a_1}{A} \sqrt{2g|h_1 - h_2|} - \frac{C_2 a_2}{A} \sqrt{2g|h_2 - H_3|} \end{bmatrix} + \begin{bmatrix} \frac{Q_1}{A} & 0 \\ 0 & \frac{Q_2}{A} \end{bmatrix} \begin{bmatrix} v_1 \\ v_2 \end{bmatrix} \quad (10)$$

Here the tanks are linked through a coupling pipe of an equivalent orifice area a_1 ; the equivalent discharging area of Tank 2 is modeled by a_2 ; the liquid level in Tank 1 is h_1 ; that in Tank 2 is h_2 with a physical constraint being $h_2 > H_3$, the equivalent height of both the coupling and discharging pipes; C_1 and C_2 are equivalent discharge constants; $A = 0.01 \text{ m}^2$ is the cross-sectional area of both tanks (which can be physically measured with a relatively high accuracy); Q_1 and Q_2 are the input flow rate per actuating volt of the Tank 1 and Tank 2 respectively; and $g = 9.81 \text{ m s}^{-2}$ the gravitational constant.

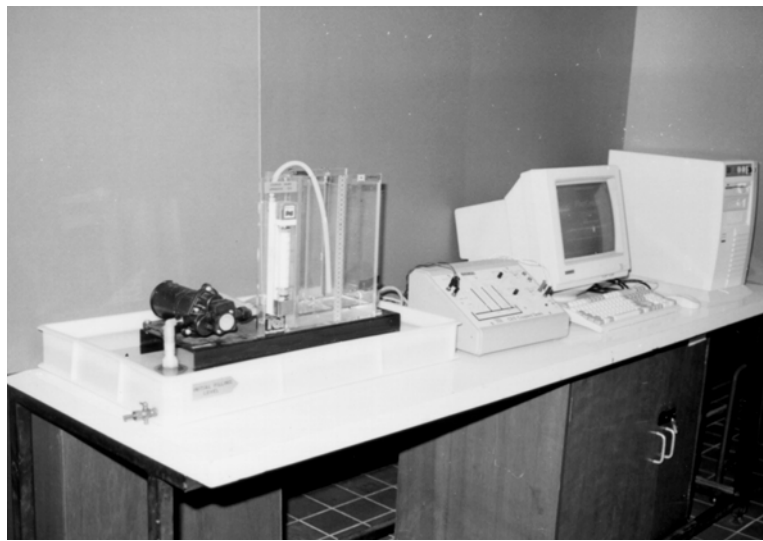


Fig. 4 A nonlinear coupled liquid tank control system

To validate the first-order model of (9), its response to the same 3 V step input has been obtained and also plotted in Fig. 3. It can be seen that the discrepancy between the model and the plant is small, but cannot be eliminated due to the limited order of the model. This problem may, however, be overcome if an infinite-order “model” is used. Convoluting the plant unit-impulse response data, $g(t) = \dot{y}_s(t)/A$, can conveniently realize such a “model” and yield a high fidelity reconstruction of the step response as shown in Fig. 3. Note that, however, the “model” may only be valid for a consistent operating point, as the steady-state gain of a linear equivalent of this nonlinear plant should not be a constant like K , but be $O(u(\infty))$.

Step response data of a plant represent a high fidelity infinite-order LTI “model”. Such a fidelity only holds at a consistent steady-state operating point if the plant is nonlinear. This opens a way of designing LTI controllers directly from plant step response data [4,29]. Of course, a more stimulating input whose spectra covers the plant bandwidth should reflect the dynamics of a practical plant more accurately. Note that this “modeling” approach may also apply to nonlinear plants for a given operating point, although a more accurate I/O relationship would be obtained by using the steady-state equilibrium and perturbing the plant round this point as adopted in linearization techniques [4]. This has eliminated the need of system identification or modeling process as required in most conventional control schemes.

B. Design Evaluation Based on Plant Step Response Data

Study Fig. 1 again, the closed-loop output contributed purely by the controlled input is given by

$$\begin{aligned} y(t) &= u(t)*g(t) = u(t)*\dot{y}_s(t) / A \\ &= [r(t) - y(t)]*h(t)*\dot{y}_s(t) / A \end{aligned} \quad (11)$$

In Laplace or Fourier transform terms, this output can be evaluated by

$$Y(j\omega) = \frac{H(j\omega)G(j\omega)}{1 + H(j\omega)G(j\omega)} \cdot R(j\omega) \quad (12)$$

where

$$G(j\omega) = \frac{j\omega Y_s(j\omega)}{A} \quad (13)$$

Therefore, given an open-loop step response, the spectra of the step response or the frequency response of a plant, the performance of an LTI controller can always be evaluated in either the time or the frequency domain without the need of a model of the plant.

V ULTIC DESIGN EXAMPLES

A. ULTIC Design for a Linear Plant Directly from Open-Loop Response Data

Without loss of generality, a typical ODE defining the time-delayed DC servomotor system for velocity control is experimented in this paper. The servo-system is given by

$$\dot{\omega}(t - .06) + \left(\frac{JR + LB}{LJ} \right) \dot{\omega}(t - .06) + \left(\frac{RB}{LJ} \right) \omega(t - .06) = \left(\frac{K_T}{LJ} \right) u(t) \quad (14)$$

where $u(t) \in [-5V, 5V]$ is the input field control voltage to reflect the saturation constraint of A/D converter; $\omega(t) \in \Re$ the angular velocity calculated from a Gray-code shaft encoder; $K_T = 13.5 \text{ NmA}^{-1}$ the torque constant for a fixed armature current; $R = 9.2 \text{ W}$ the resistance of the field winding; $B = 2.342 \times 10^3 \text{ Nms}$ the friction coefficient of the shaft; $L = 0.25 \text{ H}$ the inductance; and $J = 0.001 \text{ kgm}^2$ the moment of inertia of the motor shaft and load.

The design objective is to achieve a good closed-loop performance with excellent transient response and low chattering at the steady-state. For this, a limiting voltage of 5 V for the time-domain design or a penalized cost of $|5 - \max(u)|$ for the frequency-domain is incorporated with the performance index of (4) to limit the controller output drives within the saturation range, as well as to satisfy the various design criterion. The order of all candidate controllers is not fixed, while allowing its maximum to be third-order. Here a sampling period of 10 ms is used, as the time constant for this system is relatively small. The ULTIC controller of a minimal cost of (4) evolved directly from the step response data obtained from the physical system of (14) is given as

$$H(s) = \frac{7.2s^3 + 153.2s^2 + 426.9s + 293.8}{1.0s^3 + 27.6s^2 + 29.2s + 0.0} \quad (15)$$

It can be seen that the EA tends to provide a controller which introduces an integrator to the Type 0 system of (14). This is expected as the performance index of (4) reflects the requirement of small

steady-state errors. The EA also tends to approach a 2nd-order controller for this 2nd-order plant, as the coefficients a_3 and b_3 are relatively small. If the order of the controller is restricted to the 2nd-order, however, it will result in a high gain controller [5]. In order to test the EA designed controller, a reference given by

$$r(t) = 2Bu(t) - Bu(t-\tau) \text{ r.p.s.} \quad (16)$$

is applied, where $B = 4.5$, $u(t)$ is the unit step signal, and $\tau = 5$ s. The eddy current brake of the system is released at $t = 3$ s and reapplied at $t = 8$ s, to test the system robustness in tolerating any plant perturbations or friction disturbance. The captured closed-loop response of this system is shown in Fig. 5, which confirms that the ULTIC approach yielded a excellent transient and steady-state performance, with good robustness against the plant uncertainties.

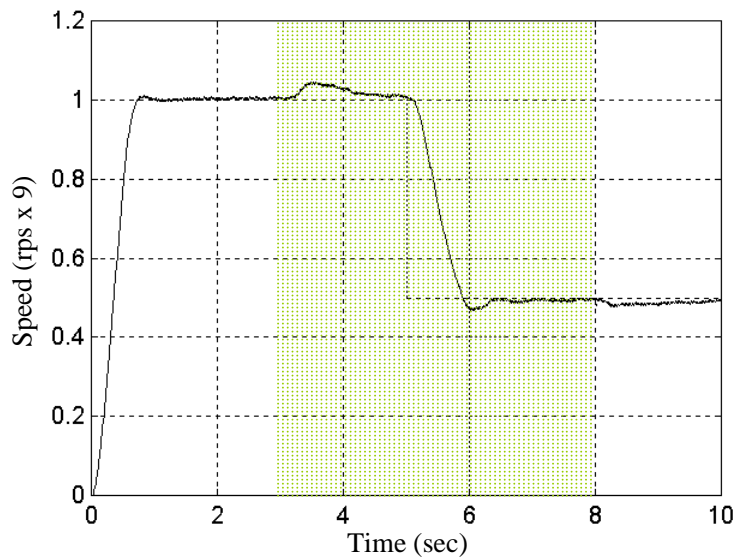


Fig. 5 Implemented performance of the I/O data evolved ULTIC system, where plant uncertainties occur at the boundaries of the shaded area

B. ULTIC Design with Emphasis on Robust Performance

Consider again the DC servo-mechanism for velocity control described in (14). The ULTIC design objective here is to achieve good robust performance of (6) and (8) in the frequency domain in order to maintain system response and error signals within pre-specified tolerances despite

uncertainties and disturbances. For this, the weighting functions W_1 and W_2 are chosen to reflect the system performance and stability robustness as given by [3,4],

$$W_1 = \frac{1}{s+1} \qquad W_2 = \frac{50(s+200)}{s+10000} \qquad (17)$$

Stability verification is carried out for every candidate controllers, such that any designs with unstable poles on the right s -plane will be assigned a predefined high cost, without performing the closed-loop simulation to reduce the overall computation time. The resulting ULTIC controller is

$$H(S) = \frac{12.46s^3 + 38.44s^2 + 44.5s + 27.68}{2.78s^3 + 3.56s^2 + 3.32s} \qquad (18)$$

Again, the EA tends to provide a controller that introduces an integrator to the Type 0 system of (14). The closed-loop response of this system for a step input of 60 r.p.m. (after a 9:1 step-down gear-box) is shown by Curve 1 in Fig. 6. To validate the robustness of the controller, a 0.2 Hz sine wave disturbance with peak-to-peak amplitude of 0.2 and 10 ms sampling period as shown by Curve 2 of Fig. 6 was applied to the system. The attenuated disturbance at the system output and the response of the motor system that suffered from this disturbance is shown by Curve 3 and Curve 4 in Fig. 6, respectively. The excellent performance clearly reveals that the specification of disturbance attenuation for the DC servo-mechanism has been met.

The resultant ULTIC controller output is shown in Fig. 7. It can be seen that the feasibility of incorporating such a practical constraint in the evolutionary design not only yields a practical control signal that offers an optimised closed-loop performance, but also eliminates the need of artificially approximating the control energy in the frequency domain [9].

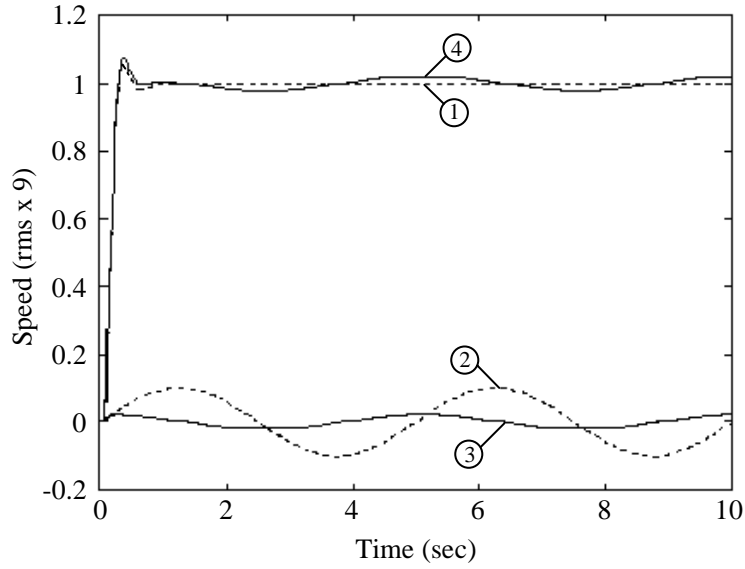


Fig. 6 Response of the step and disturbance inputs

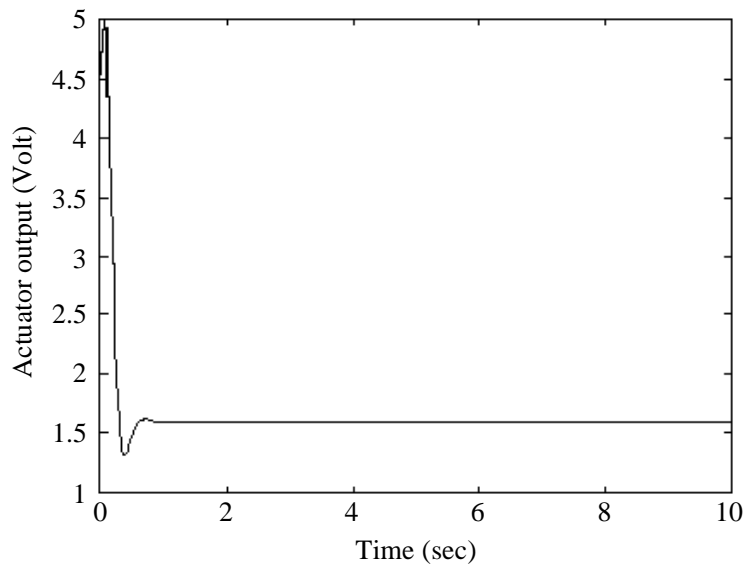


Fig. 7 Controller output with an actuator constraint of 5 volt

C. Near-Linear Pipelinability and NP of the EA

To assess the effectiveness of the parallelism, the EA design process has been repeated several times on 1, 3, 9 and 15 slave transputer(s), respectively. The average speedup is plotted in Fig. 8. It can be seen that a near-linear pipelinability is evident, which implies that evolutionary algorithms are indeed

naturally suitable for parallel processing. The other advantage of the EA approach is the non-deterministic polynomial (NP) feature, which implies that designing a more sophisticated controller would not necessarily take more time than designing a simple one. To confirm this, the design of a three-coefficient pure PID digital controller has been repeated on the same numbers of transputers. The speedup is also plotted in Fig. 8. It can be inferred that, although the number of coefficients of the third-order controller is more than doubled, it only requires an $O(n) = n \times 25\%$ increase in the design time, mainly due to the increased simulation time for the more complicated controller.

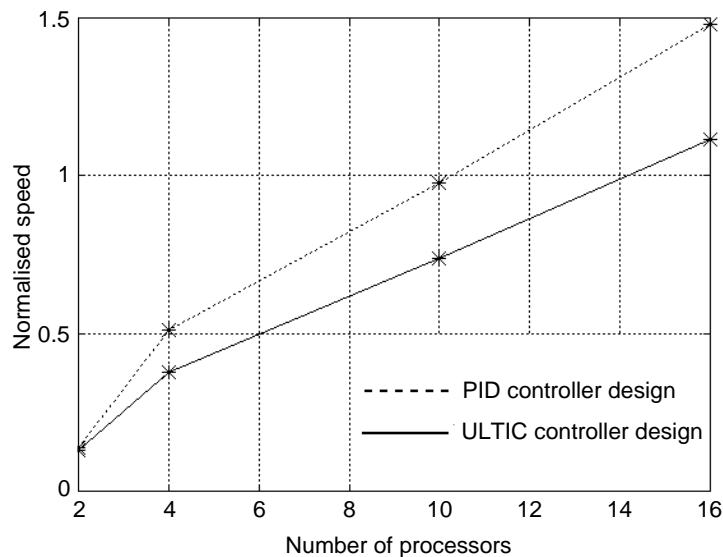


Fig. 8 The near-linear pipelinability and NP feature of the parallel EA

D. ULTIC Design for a Nonlinear Plant Directly from Open-Loop Response Data

A model representation of a nonlinear plant may sometimes be unavailable or inaccurate. By using the EA, however, an ULTIC controller can be designed directly based on the step response data from the plant, bypassing the system modeling or linearization stage. The nonlinear coupled liquid-level system in Fig. 4 is experimented here in which the nonlinearity is unseen by the EA, only the step response data in Fig. 3 is available. The ULTIC controller is designed for an operation of setting the Tank 2 liquid level to 10 cm with a quick response and rapid settlement with small steady-state errors.

The pumped inflow Q_1 is the input used to control the liquid level in Tank 2. Here, the inflow Q_2 is used as a disturbance into Tank 2 and is given by

$$Q_2(t) = 8.33 [u(t-300) - u(t-600)] \text{ cm}^3\text{s}^{-1} \quad (19)$$

The ULTIC controller designed from the EA is given by

$$H(s) = \frac{243s^3 + 151s^2 + 273s + 1.73}{1.0s^3 + 1.82s^2 + 0.44s + 0.0} \quad (20)$$

It is seen that the EA tends to supply an integrator to the Type 0 system of (10) to eliminate the steady-state error. To compare with the model-based approach, another third-order controller was designed from the identified first-order model given by (9). The resultant controller is

$$H(s) = \frac{217s^3 + 190s^2 + 299s + 1.44}{1.0s^3 + 1.81s^2 + 0.40s + 0.0} \quad (21)$$

The performances of controlling the physical coupled liquid-level system by these two controllers have been tested upon two different operating levels and added disturbances. The closed-loop step responses of Fig. 9 clearly reveals that the ULTIC designed without a model had offered a slightly better performance in controlling the nonlinear system.

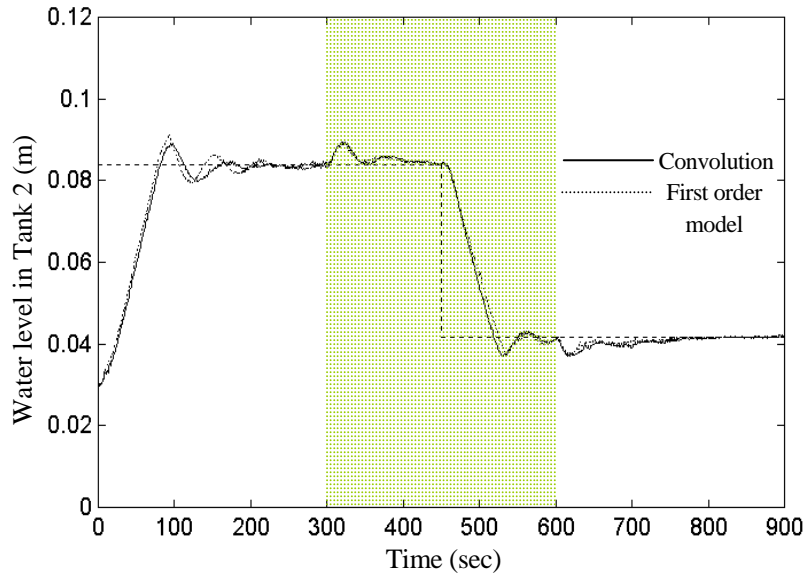


Fig. 9 The implemented performances of the ULTIC controllers designed from the I/O data and the first-order model, where disturbance occur at $t = 300$ and 600 sec

E. ULTIC Design for a MIMO Nonlinear Plant

Here, an MIMO configuration of the nonlinear couple liquid-level system of Fig. 4 is studied such that the water level of 10 cm for Tank 1 and 9 cm for Tank 2 are controlled with minimized rise-time, overshoots and steady-state errors. The input to Tank 2, Q_2 , is now the second system input. For this system, a diagonal controller would suffice [19], i.e., the controller has a transfer function matrix given by,

$$\mathbf{H} = \begin{bmatrix} H_1 & 0 \\ 0 & H_2 \end{bmatrix} \quad (22)$$

Note that the steady-state value of liquid level in Tank 1 has to be specified higher than that of Tank 2 due to the requirement of outflow of liquid in Tank 1 through Tank 2 to reach the reservoir as described by (10). Moreover, the steady-state levels of Tank 1 and Tank 2 are bounded with a maximum difference of

$$h_1(\infty) - h_2(\infty) \leq \frac{\left(\frac{Q_1}{C_1 a_1}\right)^2}{2g} \quad (23)$$

at the extreme of $Q_2 = 0$ with a given Q_1 . Similarly,

$$h_2(\infty) - H_3 \leq \frac{\left\{ \frac{C_1 a_1 \sqrt{2g(h_1(\infty) - h_2(\infty))}}{C_2 a_2} \right\}^2}{2g} \quad (24)$$

A transport delay of 1 s is found in each I/O channel of the physical system and is included in the design simulation. The obtained best diagonal ULTIC transfer function elements are

$$H_1(s) = \frac{7.9s^3 + 30.13s^2 + 95.7s + 1.02}{1.0s^3 + 0.98s^2 + 0.73s + 0.0} \quad (25)$$

$$H_2(s) = \frac{4.69s^3 + 55.76s^2 + 57.56s + 0.86}{1.0s^3 + 0.46s^2 + 0.38s + 0.0} \quad (26)$$

Implemented closed-loop response of the MIMO ULTIC control system is shown in Fig. 10. The performance clearly shows a good transient and steady-state performance. The control system also

cope well with the presence of the ‘untrained’ operating point at the step-down level. Subject to the hard voltage limit, the control signal that provides this closed-loop response is given in Fig. 11.

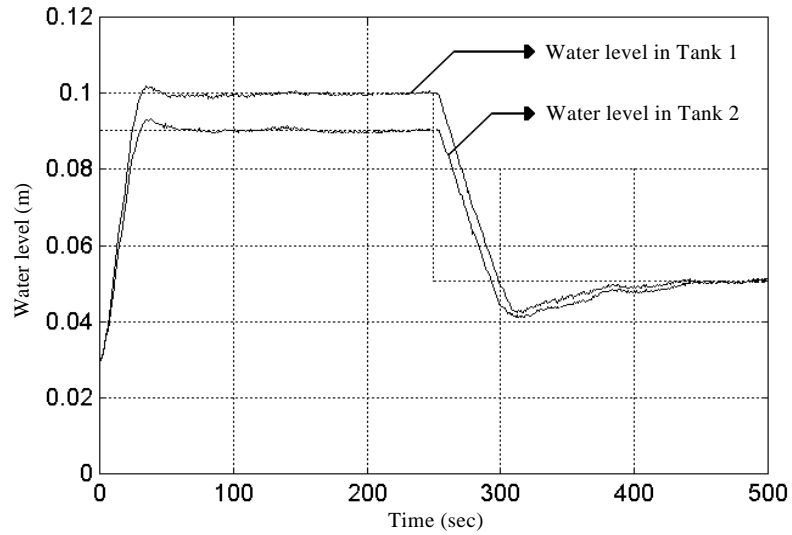


Fig. 10 Performance of the implemented MIMO ULTIC system

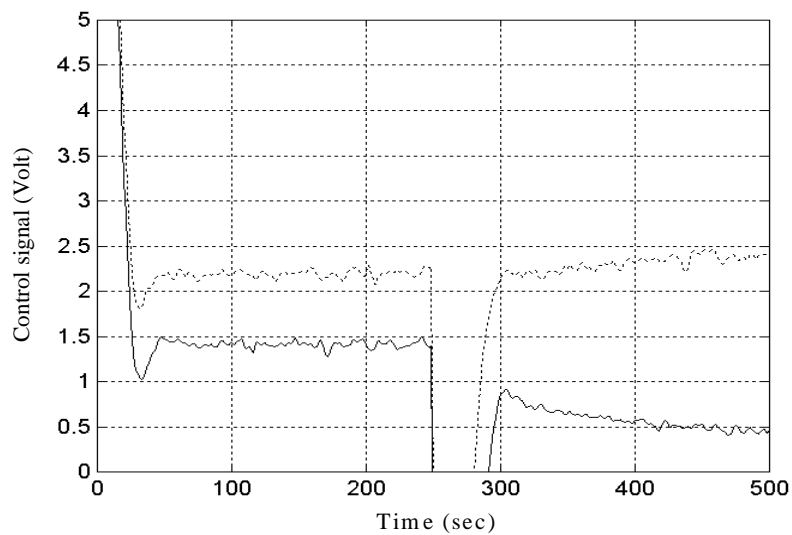


Fig. 11 Control signal of Tank 1 { — } and Tank 2 { - - - } for the MIMO ULTIC system

VI. CONCLUSIONS

In this paper, a parallel evolutionary algorithm based technique has been developed for the design unification of linear control systems in both the time and the frequency domains under performance satisfactions. A speedup of near-linear pipelinability is observed for the EA parallelism implemented on a network of Parsytec SuperCluster transputers. It is shown that the design can be further automated by efficient evolution from plant step response data, bypassing the system identification or linearization stage as required by conventional designs. Using the evolutionary ULTIC approach, control engineers only need to feed the CACSD system with the plant I/O data and customer specifications to obtain an optimal “off-the-computer” controller. In addition, the resulting ULTIC systems are easy to implement with only minor storage and computational overheads. This ULTIC design strategy has been validated against linear and nonlinear plants, with excellent performances and good robustness in the presence of constraints and perturbations.

Further work of the ULTIC methodology includes the application of multi-objective evolutionary algorithms to allow control engineers to integrate and visualize the set of performance criteria [3,30], as well as to incorporate other design objectives such as mixed-norm, controller structures and economical costing considerations.

ACKNOWLEDGEMENT

The work was partially supported by the National University of Singapore Academic Research Fund under grant NUS Project RP3981620.

REFERENCES

- [1] Y. Li, K. C. Tan, K. C. Ng and D. J. Murray-Smith, "Performance based linear control system design by genetic evolution with simulated annealing," *Proc. 34th IEEE CDC*, New Orleans, 731-7363, 1995.
- [2] Y. Li, K. C. Tan and C. Marionneau, "Direct design of uniform LTI controllers from plant I/O data using a parallel evolutionary algorithm," *Int. Conf. on Control'96, Special Session on Evolutionary Algorithms for Control Engineering*, University of Exeter, UK, 680-686, 1996.
- [3] K. C. Tan and Y. Li, "Multi-objective genetic algorithm based time and frequency domain design unification of control systems," *IFAC Int. Sym. on Artificial Intelligence in Real-Time Control*, Kuala Lumpur, Malaysia, 61-66, 1997.
- [4] K. C. Tan, *Evolutionary Methods for Modelling and Control of Linear and Nonlinear Systems*. Ph.D. Thesis, Dept. of Electronics and Electrical Eng., University of Glasgow, UK, 1997.
- [5] Y. Li, "Modern information technology for control systems design and implementation," *Proc. 2nd Asia-Pacific Conference on Control and Measurement*, Chongqing, China, pp. 17-22, 1995.
- [6] Y. Li, K. C. Ng, K. C. Tan, D. J. Murray-Smith, G. J. Gray, K. C. Sharman and E. W. McGookin, "Automation of linear and nonlinear control systems design by evolutionary computation," *Proc. IFAC Youth Automation Conf.*, Beijing, China, pp. 53-58, 1995.
- [7] A. J. Chipperfield and P. J. Fleming, "Gas turbine engine controller design using multiobjective genetic algorithms," *Proc. First IEE/IEEE Int. Conf. on GAs in Eng. Syst.: Innovations and Appl.*, Univ. of Sheffield, 214-219, 1995.
- [8] Y. Chiang and M. G. Safonov, *Robust Control Toolbox*. The MathWorks, Inc, 1992.
- [9] J. C. Doyle, B. Francis and A. Tannenbaum, *Feedback Control Theory*. Macmillan Publishing Company, New York, 1992.

- [10] Z. Michalewicz, *Genetic algorithms + Data Structure = Evolutionary Programs*. Springer-Verlag, Berlin, 2nd Edition, 1994.
- [11] D. B. Fogel, *Evolutionary Computation*. IEEE Press, Piscataway, NJ, 1995.
- [12] P. Wang and D. P. Kwok, "Auto-tuning of classical PID controllers using an advanced genetic algorithm," *Proc. 1992 Int. Conf. on Ind. Electronics, Contr., Instrumentation and Automation*, vol. 3, pp. 1224-1229, 1992.
- [13] D. P. Kwok and F. Sheng, "Genetic algorithm and simulated annealing for optimal robot arm PID control," *Proc. 1st IEEE Conf. on Evolutionary Computation, IEEE World Cong. on Computational Intelligence*, Orlando, FL, vol. 2, pp. 708-713, 1994.
- [14] K. Kristinsson and G. A. Dumont, "System identification and control using genetic algorithms," *IEEE Trans. Syst., Man and Cyber.*, vol. 22, no. 5, pp. 1033-1046, 1992.
- [15] D. P. Kwok, P. Tam, Z. Q. Sun and P. Wang, "Design of optimal linear regulators with steady-state trajectory insensitivity," *Proc. IECON 91*, vol. 3, pp. 2183-2187, 1991.
- [16] K. J. Hunt, "Polynomial LQG and H_∞ controller synthesis - A genetic algorithm solution," *Proc. 31st IEEE CDC*, Tucson, AZ, vol. 4, pp. 3604-3609, 1992.
- [17] K. J. Hunt, "Optimal controller synthesis: a genetic algorithm solution," *IEE Colloq. on Genetic Algorithms for Contr. Sys. Eng. Digest*, vol. 106, pp. 1/1-1/6, 1992.
- [18] Y. Li, K. C. Ng, D. J. Murray-Smith, K. C. Sharman and G. J. Gray, "Genetic algorithm automated approach to design of sliding mode control systems," *Int. J. of Contr.*, vol. 63, no. 4, pp. 721-739, 1996.
- [19] K. C. Ng, *Switching Control Systems and Their Design Automation via Genetic Algorithms*. Ph.D. Thesis, Dept. of Electronics and Electrical Eng., University of Glasgow, UK, 1995.
- [20] T. M. Murdock, W. E. Schmitendorf and S. Forest, "Use of genetic algorithm to analyze robust stability problems," *Proc. American Contr. Conf.*, Evanston, IL, vol. 1, pp. 886-889, 1991.

- [21] C. L. Karr, "Design of an adaptive fuzzy logic controller using a genetic algorithm," in *Genetic Algorithms: Proc. 4th Int. Conf. on Genetic Algorithms*, R. Belew, Ed., San Mateo, CA: Morgan Kaufman Publishers, pp. 450-457, 1991.
- [22] S. A. Harp and T. Samad, "Optimizing neural networks with genetic algorithms," *Proc. American Power Conf.*, Chicago IL, vol. 54, pp. 1138-1143, 1992.
- [23] Y. Li and A. Häußler, "Artificial evolution of neural networks and its application to feedback control," *Artificial Intelligence in Engineering*, vol. 10, no. 2, pp. 143-152, 1996.
- [24] G. Zames, "On the input-output stability of time-varying non-linear feedback systems," Parts I and II, *IEEE Trans. Auto. Control*, AC-11, 2 & 3, 228-238 & 465-476, 1966.
- [25] D. E. Goldberg, *Genetic Algorithms in Search, Optimization and Machine Learning*. Addison-Wesley, Reading, Massachusetts, 1989.
- [26] K. J. MacCallum, *et al.*, "Design reuse – Design concepts in new engineering contexts," *Proc. Control, Design and Production Research Conf*, Heriot-Watt Univ, 51-57, 1995.
- [27] S. Gordon and D. Whitley, "Serial and parallel genetic algorithms as function optimizers," *Proc. of the fifth Int. Conf. on Genetic Algorithms*, San Mateo, pp. 177-183, 1993.
- [28] K. J. Åström and E. Wittenmark, *Adaptive Control*. Addison-Wesley, Reading, MA, 1995.
- [29] W. R. Cluett and L. Wang, "Modelling and robust controller design using step response data," *Chemical Eng. Science*, vol. 56, pp. 2065-2077, 1991.
- [30] A. J. Chipperfield, C. M. Fonseca and P. J. Fleming, "Development of genetic optimisation tools for multi-objective optimisation problems in CACSD," *IEE Colloq. on Genetic Algorithms for Contr. Sys. Eng. Digest*, vol. 106, pp. 3/1-3/6, 1992.

Listing of Figure Captions

Fig. 1 A practical unity negative feedback control system

Fig. 2 Evolution automated CACSD by performance evaluations

Fig. 3 Plant response data $y_s(t)$ for 3 V input, response of the first-order model and response obtained by convoluting the impulse response

Fig. 4 A nonlinear coupled liquid tank control system

Fig. 5 Implemented performance of the I/O data evolved ULTIC system, where plant uncertainties occur at the boundaries of the shaded area

Fig. 6 Response of the step and disturbance inputs

Fig. 7 Controller output with an actuator constraint of 5 volt

Fig. 8 The near-linear pipelinability and NP feature of the parallel EA

Fig. 9 The implemented performances of the ULTIC controllers designed from the I/O data and the first-order model, where disturbance occur at $t = 300$ and 600 sec

Fig. 10 Performance of the implemented MIMO ULTIC system

Fig. 11 Control signal of Tank 1 { — } and Tank 2 { - - - } for the MIMO ULTIC system